Available at www.sciencedirect.com

ScienceDirect

journal homepage: www.elsevier.com/locate/he

Hydrogen storage properties of Li–Ca–N–H system with different molar ratios of $LiNH_2/CaH_2$

*Hailiang Chu, Zhitao Xiong, Guotao Wu, Teng He, Chengzhang Wu, Ping Chen**

Dalian Institute of Chemical Physics, Chinese Academy of Sciences, 457 Zhongshan Road, Dalian 116023, PR China

ARTICLE INFO

Article history:
Received 2 September 2009
Received in revised form
25 October 2009
Accepted 3 December 2009
Available online 21 December 2009

Keywords:
Lithium amide
Calcium hydride
Hydrogen desorption
Structure

ABSTRACT

In this work, dehydrogenation and rehydrogenation of three $LiNH_2/CaH_2$ samples with $LiNH_2/CaH_2$ molar ratio of 2/1, 3/1 and 4/1 were systematically investigated. Remarkable differences were observed in the temperature dependence of hydrogen desorption and subsequent absorption. $LiNH_2/CaH_2$ in a molar ratio of 2/1 transforms to ternary imide $Li_2Ca(NH)_2$ after desorbing about 4.5 wt.% H_2 at 350 °C. And it has a reversible hydrogen storage capacity of 2.7 wt.% at 200 °C. As for the $LiNH_2/CaH_2$ mixture in a molar ratio of 4/1, it transforms to a new compound with a composition of $Li_4CaN_4H_6$ after being dehydrogenated at 350 °C. The rehydrogenation of both $LiCa(NH)_2$ and $Li_4CaN_4H_6$ gives $LiNH_2$, LiH and the solid solution of $2CaNH–Ca(NH_2)_2$.

1. Introduction

Metal–N–H systems are promising candidates for hydrogen storage due to their high hydrogen content [1–10]. Li_2NH, as an example, can reversibly store about 7 wt.% of hydrogen through the following reaction pathway [1]: $Li_2NH + H_2 \leftrightarrow LiNH_2 + LiH$. However, the operating temperature for this material to release hydrogen at 1 bar equilibrium pressure is above 250 °C, which is too high to be applied on-board. Thermodynamic modification on this material is considered to be an appropriate approach to reduce the operating temperature. In recent years, such an approach has been widely adopted by different research groups to alter the thermodynamic properties of Li–N–H system [5–11]. New ternary systems, such as $LiNH_2–MgH_2$ [12,13], $LiNH_2/CaH_2$ [5,14], $LiNH_2–LiBH_4$ [15,16] and $LiNH_2–LiAlH_4$ [16–18], have been developed and characterized. Distinct changes in thermodynamic parameters have been observed. As an example, the mixture of lithium amide ($LiNH_2$) and calcium hydride (CaH_2) in a 2:1 molar ratio desorbs ~4.5 wt.% hydrogen starting at temperature as low as about 70 °C [5,14]. Though $2LiNH_2/CaH_2$ system has lower hydrogen capacity than that of $LiNH_2–MgH_2$ system, it can reversibly absorb/desorb hydrogen and has lower hydrogen desorption temperature compared with $LiNH_2–LiBH_4$ system. Such an outstanding feature enables Li–Ca–N–H an attractive system for further optimization.

In this paper, we will investigate the stoichoimetric change on the hydrogen storage properties of the Li–Ca–N–H system. Three $LiNH_2/CaH_2$ samples with $LiNH_2/CaH_2$ molar ratio of 2/1, 3/1 and 4/1 were prepared and investigated. Remarkable differences were observed in the temperature dependence of hydrogen desorption and absorption over these samples.

2. Experimental

2.1. Materials

CaH_2 with purity of 97 mass% and $LiNH_2$ with purity of 95 mass% were purchased from Sigma–Aldrich. And they were used as received.

* *Corresponding author*. Tel.: +86 411 84379905; fax: +86 411 84685940.
E-mail address: pchen@dicp.ac.cn (P. Chen).

0360-3199/$ – see front matter
doi:10.1016/j.ijhydene.2009.12.009

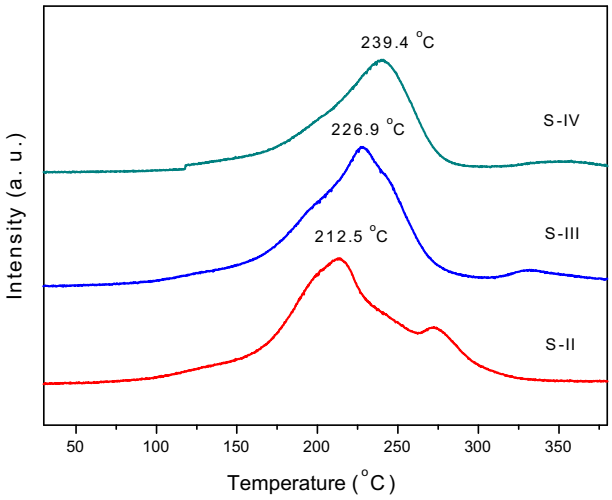

Fig. 1 – TPD-MS curves of the post-milled $CaH_2/LiNH_2$ samples.

2.2. *Sample preparation*

Three $CaH_2/LiNH_2$ samples with $LiNH_2$ to CaH_2 molar ratios of 2/1, 3/1 and 4/1, denoted as S-II, S-III and S-IV in the context, were mechanically milled using a planetary ball mill machine (Retsch, PM400) at 200 rpm. The ball milling treatment was conducted for 24 h and the ball to sample weight ratio is 30/1. The homemade milling vessel was equipped with gas valve. After the ball milling treatment, the valve was connected to a pressure gauge to measure the inner pressure. A little hydrogen gas was evolved after ball milling process. All the sample handlings were performed in the MBRAUN glove-box filled with purified argon.

2.3. *Methods*

Temperature-programmed-desorption (TPD) with purified argon as carrier gas was conducted on a homemade reactor–mass spectrometry (MS) combined system. Around 30 mg of sample was tested each time. MS was applied to detect the composition of outlet gas. At the same time, the outlet was also conducted to an ammonia (NH_3) sensitive reagent ($Co(NO_3)_2$ solution) to identify any trace of NH_3. Temperature was raised gradually from 25 °C to 380 °C at a ramping rate of 2 °C/min.

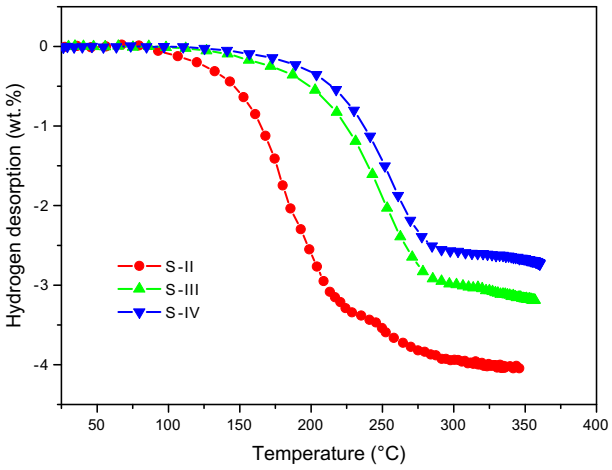

Fig. 2 – Volumetric hydrogen release from the post-milled $CaH_2/LiNH_2$ samples.

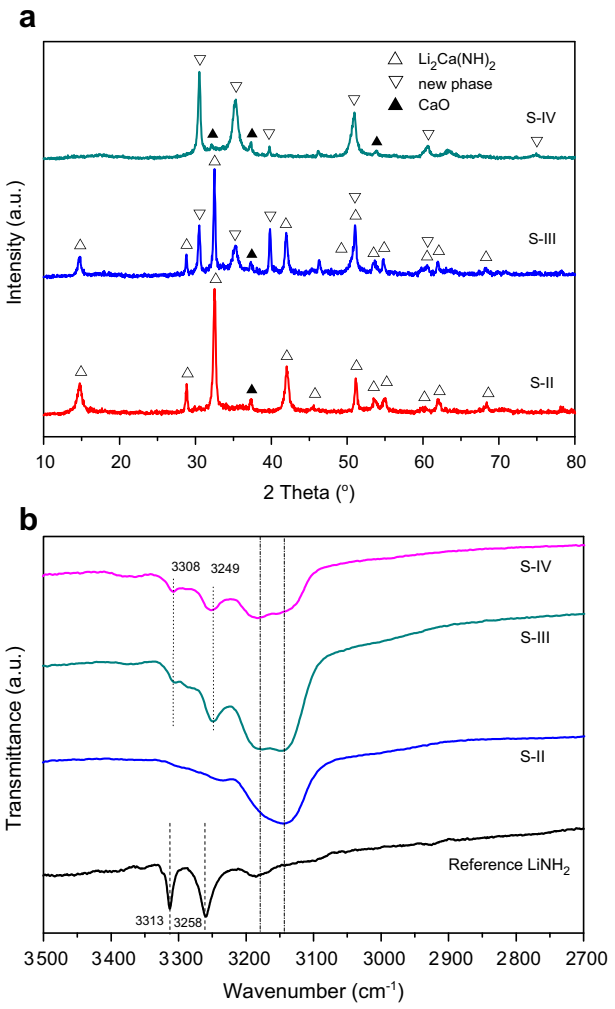

Fig. 3 – X-ray diffraction patterns (a) and FTIR spectra (b) of the samples S-II, S-III and S-IV after dehydrogenation.

XRD was performed on a Bruker D8-advance X-ray diffractometer with Cu Kα radiation at 40 kV and 40 mA and equipped with an in-situ cell. Pellets of powdery samples were made by a pellet press and placed in the in-situ cell which was subsequently evacuated to avoid contamination. The amounts of hydrogen desorption/absorption with temperature and pressure-composition isotherms (PCI) at 200 °C were measured by an automatic Sieverts-type apparatus (Advanced Materials Co.). Sample of about 500 mg was tested each time. N–H vibrations in all samples were identified by a Varian FT-IR 3000 spectroscopy in DRIFT mode.

Kissinger's approach was applied to determine activation energy involved in the hydrogen desorption from $2LiNH_2 + CaH_2$. The heating rates used were 0.5, 1, 1.5, and 2 °C/min, respectively.

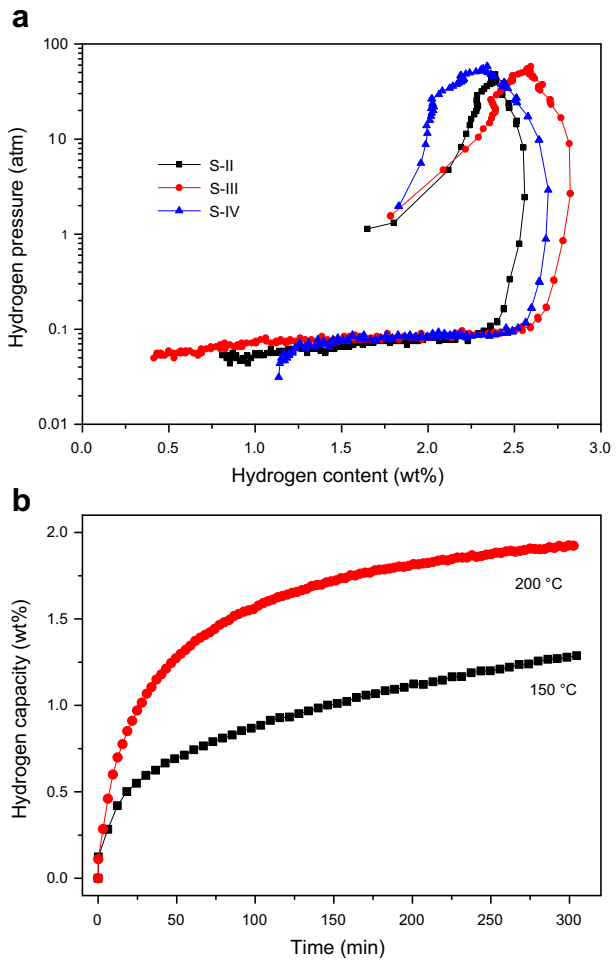

Fig. 4 – (a) PCI curves of the post-milled $CaH_2/LiNH_2$ samples and (b) Hydrogen volumetric soak of post-dehydrogenated S-II.

3. Results and discussion

Thermal desorption/decomposition of the post-milled S-II, S-III and S-IV samples were monitored by Temperature-programmed-desorption. The temperature dependences of H_2 signal detected by Mass-Spectrometer were illustrated in Fig. 1. It can be seen that hydrogen desorption starts at ~75 °C for sample S-II and at ~100 °C for the other two samples. The peak temperature of hydrogen signal increases from 212.5 °C to 239.4 °C with the increase of the molar ratio of $LiNH_2/CaH_2$. As the thermal decompositions of $LiNH_2$ and CaH_2 occur at 320 °C and 700 °C, respectively, there is chemical interaction between CaH_2 and $LiNH_2$ in the heating process. NH_3 is below the detection limit in the temperature range investigated.

By using the volumetric release method, the amount of hydrogen released can be measured quantitatively. Fig. 2 shows the temperature dependences of hydrogen desorption from the post-milled S-II, S-III and S-IV samples. The sample S-II released more hydrogen (ca. 4.0 wt. %) than the others upon heating to 350 °C. For the samples S-III and S-IV, the amount of hydrogen desorption is 3.1 and 2.7 wt.%, respectively. It should be noted that hydrogen released from the samples was gradually accumulated in the sample chamber. At the end of measurement the sample reactor was filled with hydrogen of ca. 10 psi. It is likely due to the equilibrium pressure limitation that not all hydrogen can be released from the samples.

To understand the structural change, samples after TPD measurement were collected for XRD and FTIR characterizations. As illustrated in Fig. 3(a and b), the characteristic diffraction peaks of the starting amide and hydride disappear. As for the sample II, a ternary imide $Li_2Ca(NH)_2$ is formed through the following reaction:

$$2LiNH_2 + CaH_2 \rightarrow Li_2Ca(NH)_2 + 2H_2 \quad 4.5\ wt.\% \qquad (1)$$

The new ternary imide $Li_2Ca(NH)_2$ is of a space group of $P\bar{3}m1$ and its structure has been solved by using powder X-ray diffraction [19] and neutron powder diffraction [20], respectively. A broad absorbance in the range of 3100–3200 cm^{-1} was observed (Fig. 3(b)), which corresponds to the N–H stretch in $Li_2Ca(NH)_2$. The overall absorbance of this ternary imide resembles to that of Li_2NH except the asymmetric nature caused by the presence of Ca. In the case of sample IV, the dehydrogenated solid residue exhibits a new set of diffraction at 30.5°, 35.3°, 51.0° etc. and could not be matched with any

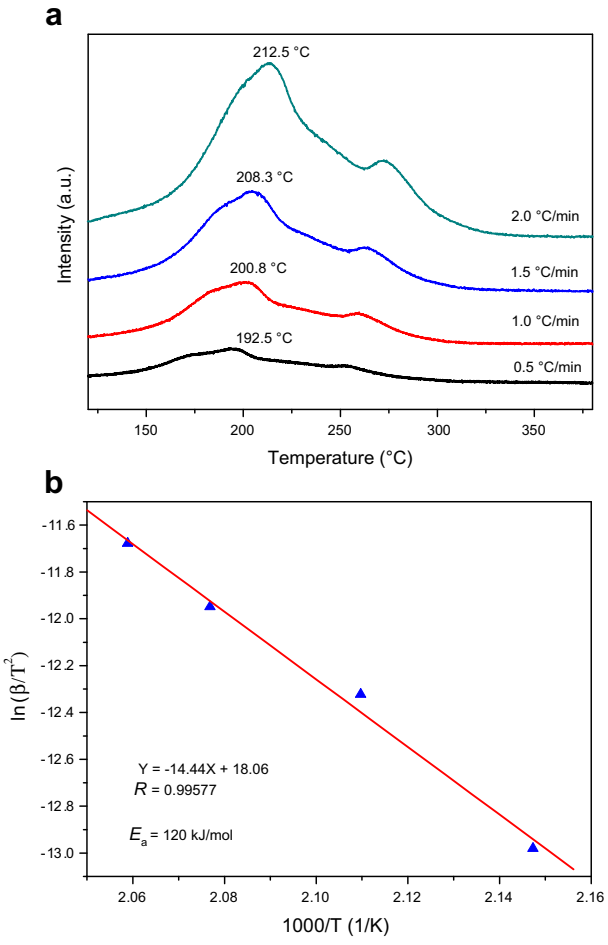

Fig. 5 – (a) TPD profiles of hydrogen desorption from the S-II and (b) Kissinger's plots.

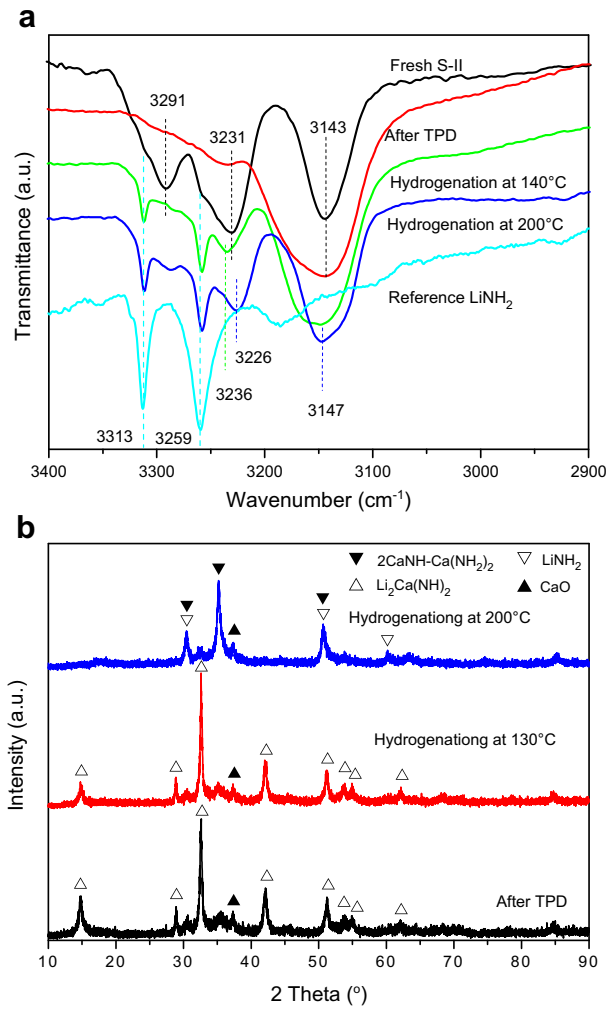

Fig. 6 – FTIR spectra (a) and X-ray diffraction patterns (b) of S-II at different states of reaction.

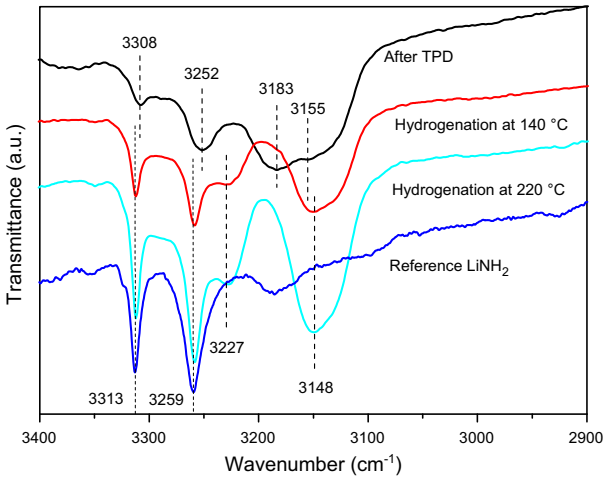

Fig. 7 – FTIR spectra of the sample S-IV at different states.

known compounds containing Li, Ca, N, and H elements. As there are 2 equiv. H_2 released from the sample S-IV, the chemical composition of the solid residue should be $Li_4CaN_4H_6$ (see reaction (2)):

$$4LiNH_2 + CaH_2 \rightarrow [Li_4CaN_4H_6] + 2H_2 \quad 3.0\ wt.\% \tag{2}$$

FTIR results showed it has four broader characteristic peaks, which are completely different from those of ternary imide $Li_2Ca(NH)_2$ and starting material $LiNH_2$. It is very likely that $Li_4CaN_4H_6$ is a single phase compound. Through the MDI Jade 5.0 software, $Li_4CaN_4H_6$ is of cubic structure with $a = 5.0964$ Å. When the molar ratio of $LiNH_2/CaH_2$ is adjusted to 3:1, XRD and FTIR results show that post-dehydrogenated sample contains both the ternary imide $Li_2Ca(NH)_2$ and $Li_4CaN_4H_6$.

To investigate the thermodynamic properties of the samples, PCI curves were measured at 200 °C and illustrated in Fig. 4(a). It can be seen that most of the hydrogen (ca. 2.5 wt.%) can be reversibly absorbed/desorbed by three samples. However, the hydrogen desorption plateau is below 0.1 atm at 200 °C, which is much lower than that of $2LiNH_2$–MgH_2 (ca. 35 atm at 200 °C) [6]. More detailed investigations are necessary to change the thermodynamic properties of Li–Ca–N–H system. Fig. 4(b) shows quantitatively the hydrogen soak over post-dehydrogenated sample S-II under ~42 atm of H_2. It can be seen that the dehydrogenated sample can absorb 1.3 wt.% and 1.9 wt.% hydrogen after about 5 h at 150 °C and 300 °C, respectively.

As the sample S-II releases more hydrogen, i.e., 4.0 wt.%, it would be interested to look at its kinetic properties. Kissinger's method was adopted in determining the activation energy:

$$d[\ln(\beta/T_m^2)/d(1/T_m)] = -E_a/R \tag{3}$$

Here T_m is the temperature at which the maximum reaction-rate peaks, β the heating rate, E_a the activation energy and R the gas constant. TPD technique was applied to collect the maximum reaction-rate temperatures at various heating rates. Fig. 5(a) summarized the TPD profiles of hydrogen desorption from the S-II at different ramping rates. It can be seen that the peak temperatures shifted monotonically to higher values when the ramping rate increased from 0.5 to 2 °C/min. The dependence of $\ln(\beta/T_m^2)$ to $1/T_m$ is plotted in Fig. 5(b). The slope of the fitted line is used to determine the value of E_a/R. Thus, the activation energy for hydrogen desorption from the S-II is around 120 kJ/mol, which is slightly higher than that of $2LiH$–$Mg(NH_2)_2$ system [11].

The structural change of the sample S-II in the hydrogenation/dehydrogenation was investigated. Fig. 6(a) shows FTIR spectra of $2LiNH_2/CaH_2$ mixture at different states. For the fresh sample, two peaks at 3291 and 3231 cm^{-1} are observed, which are completely different from those of the starting material $LiNH_2$ and can be assigned to $Ca(NH_2)_2$, evidencing that the formation of $Ca(NH_2)_2$ upon ball milling $2LiNH_2$ and CaH_2 because a cation exchange should take place in the milling process. On the other hand, a broad peak centered at 3143 cm^{-1} was detected, which can be assigned to the stretch of the N–H bond in ternary imide $Li_2Ca(NH)_2$ formed during ball milling treatment. It can be verified by the evolution of hydrogen gas during ball milling process. After the TPD treatment, amide peaks (at 3291 and 3231 cm^{-1}) disappear, and only

the broad imide peak at 3143 cm^{-1} can be observed. Subsequently, the sample was re-hydrogenated at 130 °C, 140 °C and 200 °C overnight, respectively. However, the sample cannot be hydrogenated at 130 °C according to the XRD observation (Fig. 6(b)). After being hydrogenated at 140 °C, the sample presents two peaks at 3313 and 3259 cm^{-1} showing the regeneration of lithium amide. After being hydrogenated at 200 °C, FTIR results show that, except the two peaks of $LiNH_2$, another two new peaks at around 3226 cm^{-1} and 3147 cm^{-1} are observed, which can be assigned to a solid solution of $Ca(NH_2)_2$ and CaNH. According to the previous published results [21], the composition of the solid solution was $2CaNH–Ca(NH_2)_2$. XRD pattern of the sample II after being hydrogenated at 200 °C (Fig. 6(b)) displays identical pattern as that reported in literature [21] except for $LiNH_2$. Take into consideration of FTIR and XRD measurements, the hydrogenation process of ternary imide $Li_2Ca(NH)_2$ can be expressed as reaction (4):

$$Li_2Ca(NH)_2 + 5/3H_2 \rightarrow 2/3LiNH_2 + 4/3LiH + 1/3[2CaNH–Ca(NH_2)_2] \quad (4)$$

As for the sample S-IV, the FTIR observations at different hydrogenation stages are shown in Fig. 7, which present similar occurings as that of S-II, i.e., $LiNH_2$ (at 3313 and 3259 cm^{-1}) and solid solution $2CaNH–1Ca(NH_2)_2$ (at around 3227 cm^{-1} and 3148 cm^{-1}) are formed upon hydrogenation at 140 °C and above. Together with the amount of hydrogen absorbed, the reaction (5) can be used to describe the hydrogenation of S-IV.

$$[Li_4CaN_4H_6] + 4/3H_2 \rightarrow 8/3LiNH_2 + 4/3LiH + 1/3[2CaNH–Ca(NH_2)_2] \quad (5)$$

4. Conclusion

The hydrogen storage and structural properties of the Li–Ca–N–H system, which with different $LiNH_2/CaH_2$ molar ratios have been systematically investigated. It was found that $2LiNH_2/CaH_2$ has better hydrogen storage properties. Its reversible hydrogen storage reaction can be expressed as follows: $2LiNH_2 + CaH_2 \rightarrow Li_2Ca(NH)_2 + 2H_2 \rightarrow 2/3LiNH_2 + 4/3LiH + 1/3[2CaNH–Ca(NH_2)_2] + 1/3H_2$. It can desorbs 4.0 wt.% hydrogen at 350 °C and the reversible hydrogen storage capacity can reach 2.7 wt.% at 200 °C. However, the activation energy ($E_a = 120$ kJ/mol) of releasing hydrogen is relatively large. With increasing $LiNH_2/CaH_2$ molar ratio to 4:1, a new compound with the composition of $Li_4CaN_4H_6$ is formed. The reversible hydrogen storage reaction can be expressed as follows: $4LiNH_2 + CaH_2 \rightarrow [Li_4CaN_4H_6] + 2H_2 \rightarrow 8/3LiNH_2 + 4/3LiH + 1/3[2CaNH–Ca(NH_2)_2] + 2/3H_2$.

Acknowledgement

This work was financially supported by the National High Technology Research and Development Program (863 Program) of China (No. 2009AA05Z108) and the Hundred Talents Projects of CAS (No. KGCX2-YW-806).

REFERENCES

[1] Chen P, Xiong ZT, Luo JZ, Lin JY, Tan KL. Interaction of hydrogen with metal nitrides and imides. Nature 2002;420:302–4.
[2] Osborn W, Markmaitree T, Shaw LL, Hu JZ, Kwak J, Yang ZG. Low temperature milling of the $LiNH_2 + LiH$ hydrogen storage system. Int J Hydrogen Energy 2009;34:4331–9.
[3] Ikeda S, Kuriyama N, Kiyobayashi T. Simultaneous determination of ammonia emission and hydrogen capacity variation during the cyclic testing for $LiNH_2$–LiH hydrogen storage system. Int J Hydrogen Energy 2008;33:6201–4.
[4] Chen P, Zhu M. Recent progress in hydrogen storage. Mater Today 2008;11:36–43.
[5] Xiong ZT, Wu GT, Hu JJ, Chen P. Ternary imides for hydrogen storage. Adv Mater 2004;16:1522–5.
[6] Luo WF. ($LiNH_2$–MgH_2): a viable hydrogen storage system. J Alloys Compd 2004;381:284–7.
[7] Leng HY, Ichikawa T, Hino S, Hanada N, Isobe S, Fujii H. New metal–N–H system composed of $Mg(NH_2)_2$ and LiH for hydrogen storage. J Phys Chem B 2004;108:8763–5.
[8] Nakamori Y, Orimo S. Destabilization of Li-based complex hydrides. J Alloys Compd 2004;370:271–5.
[9] Pinkerton F, Mersner G, Meyer M, Balogh M, Kundrat M. Hydrogen desorption exceeding ten weight percent from the new quaternary hydride $Li_3BN_2H_8$. J Phys Chem B 2005;109:6–8.
[10] Markmaitree T, Osborn W, Shaw LL. Comparisons between MgH_2- and LiH-containing systems for hydrogen storage applications. Int J Hydrogen Energy 2008;33:3915–24.
[11] Xiong ZT, Hu JJ, Wu GT, Chen P, Luo WF, Gross K, et al. Thermodynamic and kinetic investigations of the hydrogen storage in the Li–Mg–N–H system. J Alloys Compd 2005;398:235–9.
[12] Shahi RR, Yadav TP, Shaz MA, Srivastava ON. Effects of mechanical milling on desorption kinetics and phase transformation of $LiNH_2/MgH_2$ mixture. Int J Hydrogen Energy 2008;33:6188–94.
[13] Chen Y, Wu CZ, Wang P, Cheng HM. Structure and hydrogen storage property of ball-milled $LiNH_2/MgH_2$ mixture. Int J Hydrogen Energy 2006;31:1236–40.
[14] Tokoyoda K, Hino S, Ichikawa T, Okamoto K, Fujii H. Hydrogen desorption/absorption properties of Li–Ca–N–H system. J Alloys Compd 2007;439:337–41.
[15] Meisner GP, Scullin ML, Balogh MP, Pinkerton FE, Meyer MS. Hydrogen release from mixtures of lithium borohydride and lithium amide: a phase diagram study. J Phys Chem B 2006;110:4186–92.
[16] Nakamori Y, Ninomiya A, Kitahara G, Aoki M, Noritake T, Miwa K, et al. Dehydriding reactions of mixed complex hydrides. J Power Sources 2006;155:447–55.
[17] Xiong ZT, Wu GT, Hu JJ, Chen P. Investigation on chemical reaction between $LiAlH_4$ and $LiNH_2$. J Power Sources 2006;159:167–70.
[18] Xiong ZT, Wu GT, Hu JJ, Liu YF, Chen P, Luo WF, et al. Reversible hydrogen storage by a Li–Al–N–H complex. Adv Funct Mater 2007;17:1137–42.
[19] Wu GT, Xiong ZT, Liu T, Liu YF, Hu JJ, Chen P, et al. Synthesis and characterization of a new ternary imide – $Li_2Ca(NH)_2$. Inorg Chem 2007;46(2):517–21.
[20] Wu H. Structure of ternary imide $Li_2Ca(NH)_2$ and hydrogen storage mechanisms in amide–hydride system. J Am Chem Soc 2008;130:6515–22.
[21] Xiong ZT, Wu GT, Hu JJ, Chen P. Ca–Na–N–H system for reversible hydrogen storage. J Alloys Compd 2007;441:152–6.